

# Combining Datasets with Different Label Sets for Improved Nucleus Segmentation and Classification

Amruta Parulekar<sup>1,\*</sup>, Utkarsh Kanwat<sup>1,\*</sup>, Ravi Kant Gupta<sup>1</sup>, Medha Chippa<sup>1</sup>, Thomas Jacob<sup>1</sup>,  
Tripti Bameta<sup>2</sup>, Swapnil Rane<sup>2</sup> and Amit Sethi<sup>1</sup>

<sup>1</sup>Indian Institute of Technology, Bombay, Mumbai, India

<sup>2</sup>Tata Memorial Centre-ACTREC (HBNI), Mumbai, India

**Keywords:** Cell Nuclei, Classification, Histopathology, Segmentation.

**Abstract:** Segmentation and classification of cell nuclei using deep neural networks (DNNs) can save pathologists' time for diagnosing various diseases, including cancers. The accuracy of DNNs increases with the sizes of annotated datasets available for training. The available public datasets with nuclear annotations and labels differ in their class label sets. We propose a method to train DNNs on multiple datasets where the set of classes across the datasets are related but not the same. Our method is designed to utilize class hierarchies, where the set of classes in a dataset can be at any level of the hierarchy. Our results demonstrate that segmentation and classification metrics for the class set used by the test split of a dataset can improve by pre-training on another dataset that may even have a different set of classes due to the expansion of the training set enabled by our method. Furthermore, generalization to previously unseen datasets also improves by combining multiple other datasets with different sets of classes for training. The improvement is both qualitative and quantitative. The proposed method can be adapted for various loss functions, DNN architectures, and application domains.

## 1 INTRODUCTION

Histopathology is practice of preparation and observation of tissue slides to visually identify signs and grades of various diseases, including cancers. The visual features include nucleus to cytoplasm ratio, nuclear pleomorphism, and counts of various types of cells. Usually histopathological examination relies on nuclear details for estimating these features as the cell (cytoplasmic) boundaries are not easy to identify in hematoxylin and eosin (H&E) stained samples, which is a staple of histopathology. Automating instance segmentation and classification of nuclei using deep neural networks (DNNs), such as HoVerNet (Graham et al., 2019) and StarDist (Schmidt et al., 2018) on whole slide images (WSIs) acquired using scanners, can bring efficiencies and objectivity to several types of histological diagnostic and prognostic tasks.

Because DNNs can be scaled to generalize better with more diverse and larger datasets, it is necessary to accurately annotate and label multiple large datasets for their training. In the last few years,

several annotated histological datasets have been released that differ in the sets of nuclear class labels, magnification, source hospitals, scanning equipment, organs, and diseases. For instance, while the PanNuke dataset covers 19 organs with semi-automated annotation of five nuclear classes – neoplastic, non-neoplastic epithelial, inflammatory, connective, dead (Gamper et al., 2020); the MoNuSAC covers four organs with the following four nuclear classes – epithelial, lymphocytes, macrophages, and neutrophils (Verma et al., 2021). While most of this input diversity is beneficial to train generalized DNNs, combined training across datasets with different sets of class labels remains a challenge. Existing methods to train DNNs on multiple datasets that differ class label sets are not satisfactory. For instance, transfer (Yosinski et al., 2014) and multi-task learning (Zhang et al., 2014), do not train the last (few) layer(s) of a DNN on more than one dataset.

We propose a method to train DNNs for instance segmentation and classification over multiple related datasets for the same types of objects that have different class label sets. Specifically, we make the following contributions. (1) We propose a method to mod-

\*These authors contributed equally to this work

Table 1: Characteristics of notable nucleus segmentation and classification datasets.

Dataset	Classes	Organs	Mag.	Nuclei	Images	Img. Size
PanNuke (Gamper et al., 2020)	5: Inflammatory, Neoplastic, Dead, Connective, Non-neoplastic Epithelial	19: Bladder, Ovary, Pancreas, Thyroid, Liver, Testis, Prostrate, Stomach, Kidney, Adrenal gland, Skin, Head & Neck, Cervix, Lung, Uterus, Esophagus, Bile-duct, Colon, Breast	40x	216,345	481	224x224
MoNuSAC (Verma et al., 2021)	4: Epithelial, lymphocytes, macrophages, neutrophils	4: Breast, Kidney, Liver, prostrate	40x	46,909	310	82x35 to 1422x2162
CoNSeP (Graham et al., 2019)	7: Healthy Epithelial, Inflammatory, Muscle, Fibroblast, Malignant Epithelial, Endothelial, Other	1: Colon	40x	24,319	41	1000x1000

ify a wide variety of loss functions used for segmentation and classification. (2) The method is applicable whenever the class label sets across the datasets can be expressed as a part of a common coarse-to-fine class hierarchy tree. That is, the method can jointly utilize multiple datasets of the same types of objects wherein some datasets may have labels for finer sub-classes while others may have labels for coarser super-classes, or a mix of these, from the same class hierarchy tree. Apart from this type of relation among datasets, the method has no other constraints. That is, it can be used to train a wide variety of DNNs for instance segmentation and classification for various types of objects of interest, although we used the segmentation of nuclei in histopathology using StarDist (Schmidt et al., 2018) as a case study. (3) We demonstrate quantitative and qualitative improvements in nuclear segmentation and classification test accuracy using the proposed method to train on multiple datasets with different class label sets. (4) We also show that thus using multiple datasets also improves domain generalization on a previously unseen dataset.

## 2 RELATED WORKS

In this section, we review nucleus segmentation datasets and methods, and previous attempts to combine knowledge from multiple datasets.

Over the last few years, several datasets with careful annotations and labeling of cell nuclei have been released to the public to enable research on better instance segmentation and classification models. Some notable datasets are shown in Table 1. These datasets

meet our goals as they contain images with nuclear details at 40x magnification and labels for nuclei from multiple classes, unlike, for example, MoNuSeg (Kumar et al., 2017) or CryoNuSeg (Mahbod et al., 2021).

Research on nucleus segmentation and classification methods has recently seen the development of combination architectures (fusion of multiple networks) and specialized architectures. For instance, HoVerNet (Graham et al., 2019) was proposed to predict whether a pixel location is inside a nucleus and its horizontal and vertical distances from the nuclear boundary. This concept has been generalized to predict multi-directional distance using StarDist (Schmidt et al., 2018). These architectures are specifically designed for histological images with overcrowded nuclei and have demonstrated state-of-the-art results compared to previous methods.

In order to combine knowledge from multiple datasets, transfer and multi-task learning have been proposed for natural and medical images. For instance, (Reis and Turk, 2023) proposes a transfer learning technique using the MedCLNet database. DNNs were pre-trained through the proposed method and were used to perform classification on the colorectal histology MNIST dataset. The GSN-HVNET (Zhao et al., 2023) was proposed with an encoder-decoder structure for simultaneous segmentation and classification of nuclei, and was pre-trained on the PanNuke dataset.

Although coarse-to-fine class structure has been exploited for knowledge transfer in other domains (Li et al., 2019), it has not been used in medical datasets for increasing the data for training or domain generalization.

All the methods described so far have only dealt

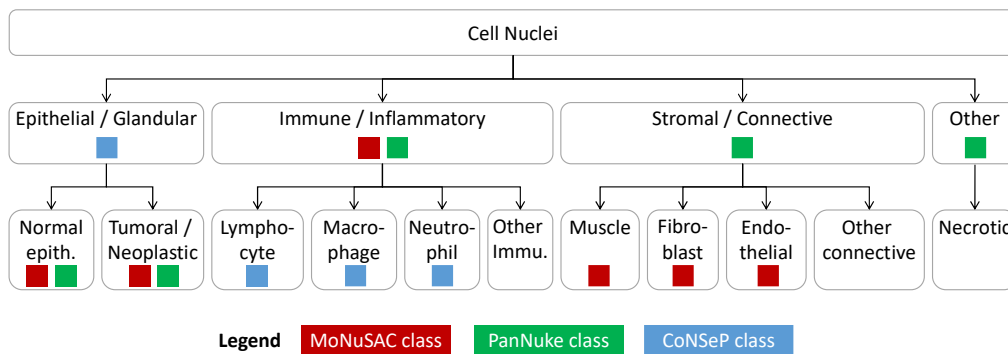


Figure 1: Hierarchy of nucleus classes and their correspondence to the three label sets of the datasets used in this study.

with the scenario of carrying out segmentation and classification by splitting the same dataset into training and testing, or using the same set of classes across training and testing. At best, transfer learning was carried out where only the lower pretrained layers were retained and new upper layers were randomly initialized and trained on target datasets. There are no loss functions or training methods that can train an all layers of a DNN on multiple datasets for cross-domain (dataset) generalization for segmentation and classification.

### 3 PROPOSED METHOD

We propose a method to train DNNs for segmentation and classification on multiple datasets with related but potentially different class label sets. We assume that the class label sets across the datasets are different cuts of the same class hierarchy tree. Within each dataset, the class labels are mutually exclusive, but need not be collectively exhaustive. An example of a class hierarchy tree with different cuts for labels for three different datasets is given in Figure 1, where nuclei can be divided into four super-classes, which in turn can be divided into 11 sub-classes. Deeper and wider hierarchies can also be used. Class label sets that are not a part of a common class hierarchy tree are out of the scope of this work.

Our key idea is to modify a class of loss functions whose computation involves sums over predicted and ground truth class probability terms in conjunction with sums over instances or pixels. This description covers a wide array of loss functions, including cross entropy, Dice loss (Sudre et al., 2017), focal loss (Lin et al., 2017), Tversky loss, focal Tversky loss (Abraham and Khan, 2018). We propose to sum the predicted probabilities of fine-grained sub-classes when the class label is only available at their coarser super-class level. The set of finer sub-classes

to be combined using this method of loss computation can even dynamically change from dataset-to-dataset, epoch-to-epoch, batch-to-batch, or even instance-to-instance. To keep things simple, we first train the model on one dataset for a few epochs, and then train it on a second dataset for the remaining epochs.

This method is also applicable to any DNN architecture or application domain (e.g., natural images) that can be trained using these losses. As a case study, we use it to modify cross entropy and focal Tversky loss functions (Abdohoseini et al., 2019) to train a UNet-based StarDist DNN (Schmidt et al., 2018) for H&E-stained histopathology nucleus segmentation and classification on MoNuSAC (Verma et al., 2021), PanNuke (Gamper et al., 2020), and CoNSEP (Graham et al., 2019) datasets.

Although this method can be extended to multiple levels, for simplicity of explanation we will assume that a class label can be at one of the two levels – a super-class or a sub-class. We design a neural architecture that makes predictions at the finest level of the hierarchy, which is the set of all sub-classes (plus background) in this case. When the label for a training instance is available at the super-class level, we add the predicted probabilities of its sub-classes, and update their weights with an equal gradient, as should be done backwards of a sum node. This way, the weights leading to the prediction of all sub-classes are trained even when only the super-class label is available. The gradient and output obtained from this approach is at the finest (sub-class) level, but we interpret the results for a dataset only for its corresponding training label set. That is, we do not assess sub-class level performance when only super-class labels are available, even though we train the DNN to predict at the sub-class level. On the other hand, when we come across a training instance where a sub-class label is available, we skip the sum-based merging of probability masses. In this case, class-specific weight update and the interpretation of predictions proceeds in the usual

fashion.

Consider the cross entropy loss for a fixed set of class labels:

$$L_{CE} = - \sum_{i=1}^n \sum_{j=1}^c t_{ij} \log(y_{ij}), \quad (1)$$

where  $n$  is the number of training instances,  $c$  is the number of classes,  $t_{ij}$  are one-hot labels, and  $y_{ij}$  are the predicted class probabilities such that  $\forall i \sum_j t_{ij} = 1, \sum_j y_{ij} = 1$ . In case a subset of classes belong to a super-class  $k$  denoted by  $j \in S_k$ , then we modify Equation 1 as follows:

$$L_{MCE} = - \sum_{i=1}^n \sum_{k=1}^m t_{ik} \log y_{ik} = - \sum_{i=1}^n \sum_{k=1}^m t_{ik} \log \left( \sum_{j \in S_k} y_{ij} \right), \quad (2)$$

where  $t_{ik}$  is a binary indicator label for the super-class  $k$ , and  $m$  is the size of the class label set. That is,  $t_{ik} = \sum_{j \in S_k} t_{ij}$ , but the individual terms  $t_{ij}$  may not be known in the given labels. The class probability predictions  $y_{ij}$  can remain at the finest level across datasets, while the labels  $t_{ik}$  can be at the finest or a coarser level. Just as it was the case for the labels, the predicted probabilities also naturally satisfy the relation  $y_{ik} = \sum_{j \in S_k} y_{ij}$ . As is clear from Equation 2, that although for notational simplicity, the sum over classes runs at the super-classes enumerated by  $k$  at the same level, the modification applies independently to each branch of the class hierarchy tree (see Figure 1 for an example), as was done in our implementation. Additionally, it is also clear that the method can be extended to deeper and wider hierarchy trees with label sets that are arbitrary cuts of the tree.

We next consider a slightly more complex loss – the focal Tversky loss (Abraham and Khan, 2018):

$$L_{FT} = \sum_{i=1}^n \left( 1 - \frac{\sum_{j=1}^c (t_{ij} y_{ij} + \epsilon)}{\alpha \sum_{j=1}^c t_{ij} + (1 - \alpha) \sum_{j=1}^c y_{ij} + \epsilon} \right)^\gamma, \quad (3)$$

where  $\epsilon$  is a small constant to prevent division by 0, and  $\alpha > 0, \gamma > 0$  are hyper-parameters. Following the same principles as used to propose the loss in Equation 2, we now propose a modified focal Tversky loss:

$$L_{MFT} = \sum_{i=1}^n \left( 1 - \frac{\sum_{k=1}^m (t_{ik} \sum_{j \in S_k} y_{ij} + \epsilon)}{\alpha \sum_{k=1}^m t_{ik} + (1 - \alpha) \sum_{k=1}^m \sum_{j \in S_k} y_{ij} + \epsilon} \right)^\gamma. \quad (4)$$

Once again, it is clear that  $L_{MFT}$  can also be modified to be applied independently to each branch and sub-branch of a class hierarchy tree, including labels at different levels of the tree that are in different branches.

In our implementation of nuclear instance segmentation and classification, we used a positive combination of  $L_{MCE}$  and  $L_{MFT}$ .

## 4 EXPERIMENTS AND RESULTS

We tested two hypotheses in our experiments. Firstly, we hypothesized that using the proposed method, pre-training on a related source dataset A with class labels derived from the same class hierarchy tree as that of a target dataset B can improve the instance segmentation and classification metrics on the held-out test cases of dataset B compared to training only on dataset B. Secondly, we hypothesized that using the proposed method, domain generalization to a previously unseen dataset C can improve when trained on datasets A and B, as compared to training only on dataset B, where the label sets for the three datasets may be different but are derived from the same class hierarchy tree. For experiments to confirm either hypotheses, we did not discard the last (few) layer(s) after training on dataset A, as is done in transfer learning and multi-task learning. We trained, retained, and re-trained the same last layer by using the proposed adaptive loss functions.

Due to their large size, 40x magnification with clear nuclear details, and a minimal overlap in nuclear classes, we selected three datasets for our experiments – the Multi-organ Nuclei Segmentation And Classification (MoNuSAC) (Verma et al., 2021) dataset, the PanNuke dataset (Gamper et al., 2020), and the Colorectal Nuclear Segmentation and Phenotypes (CoN-SeP) dataset (Graham et al., 2019). More details about these datasets can be found in Section 2.

Due to its integrated evaluation of instance segmentation and classification, we used panoptic quality (PQ) (Kirillov et al., 2019) to assess our results.

This metric is now widely used as the primary metric in papers such as (Weigert and Schmidt, 2022) for assessing nucleus segmentation and classification. (Kirillov et al., 2019) shows rigorous experimental evaluation that demonstrates the variation of PQ, along with its comparison to other metrics like intersection over union (IoU) and average precision (AP)

We used an instance segmentation and classification architecture used in (Weigert and Schmidt, 2022) (which is a modification of the StarDist (Schmidt et al., 2018) model) because it has specific training procedures and post-processing steps for H&E-stained histology images. It also gives enhanced object localization, leading to higher precision in segmentation, especially of overlapping or closely located nuclei.



Patches of size 256x256 were extracted from each dataset. Smaller images were appropriately padded. Some patches were overlapping while others were cut-off to fit within 256x256. Images had three channels corresponding to RGB. The ground truth masks had two channels – the first was the instance segmentation map ranging from 0 to number of nuclei and the second was the classification map ranging from zero to number of classes in the dataset’s class label set.

To combat staining variability, random brightness, hue, and saturation augmentations were performed on the images. To combat class imbalance, geometric augmentations (90 degree rotations and flips) and elastic augmentations were performed more frequently on the less populated classes.

The optimizer used was Adam. We monitored the validation loss for early stopping. Once we finished training the model on one dataset (dataset A) using one instantiation of the modified loss function for a few epochs, we further trained (finetuned) the same model - without adding or removing any layers or weights - on the second dataset (dataset B) for a few more epochs by adapting the loss to the second day. The method is flexible enough to take training instances from multiple datasets down to batch-level, but we simplified the procedure to keep the training consistent at an episode (group of epochs) level, where only one dataset was used for training per episode.

#### 4.1 Test Dataset Results

Table 2 summarizes the results of testing the first hypothesis that the test results can improve by pre-training on another dataset using the proposed method. Pre-training on another dataset and then fine-tuning for a small number of epochs (Eps) on our target dataset consistently gave better results for all three target datasets as compared to training only on the target dataset. Additionally, these results compare favorably with the state-of-the-art for training and testing on various splits of a single dataset (Schmidt et al., 2018).

Table 3 shows that we have achieved state-of-the-art panoptic quality value on the CoNSeP dataset with our proposed method, pretrained on PaNNuke and fine-tuned on CoNSeP. For MoNuSAC, we find that our method surpasses the Unet (Ronneberger et al., 2015), DeepLabV3 (Chen et al., 2017) and PSPNet (Zhao et al., 2017) models, which have PQ values of 0.350, 0.396, and 0.387, respectively.

A sample of qualitative results shown in Figure 2 also shows better overlap between predicted nuclei and annotations for test images when multiple train-

Table 2: Quantitative results on test splits.

Pre-Train	Eps	Fine-tune	Eps	Test	PQ
CoNSeP	100	-	-	CoNSeP	0.540
MoNuSAC	175	CoNSeP	75	CoNSeP	<b>0.555</b>
PanNuke	250	CoNSeP	75	CoNSeP	<b>0.571</b>
MoNuSAC	175	-	-	MoNuSAC	0.579
CoNSeP	100	MoNuSAC	130	MoNuSAC	<b>0.587</b>
PanNuke	250	MoNuSAC	130	MoNuSAC	<b>0.602</b>
PanNuke	250	-	-	PanNuke	<b>0.610</b>
CoNSeP	100	PanNuke	187	PanNuke	0.605
MoNuSAC	175	PanNuke	187	PanNuke	<b>0.610</b>

Table 3: Comparison of results with existing models for CoNSeP dataset. Best result is highlighted as bold.

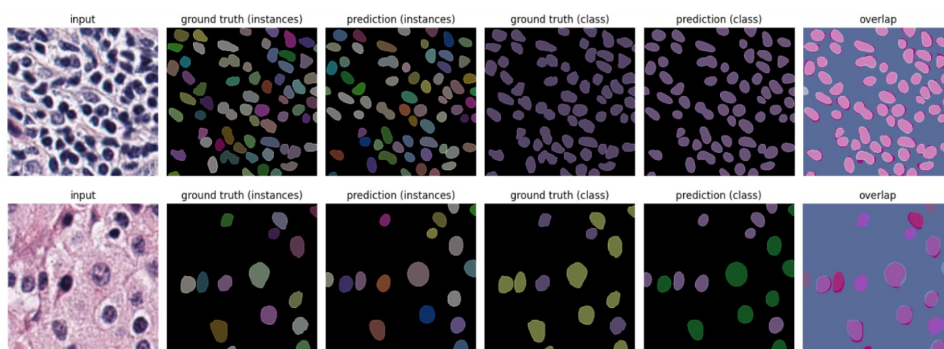
Model	PQ	Model	PQ
UNet++ (Zhou et al., 2018)	0.405	DSCANet (Ye et al., 2024)	0.426
DiffMix (Oh and Jeong, 2023)	0.505	GradMix (Doan et al., 2022)	0.504
Hovernet (Graham et al., 2019)	0.532	SMILE (Pan et al., 2023)	0.530
DRCANet (Dogar et al., 2023)	0.546	DeepLabV3+ (Chen et al., 2017)	0.373
Stardist (Schmidt et al., 2018)	0.540	Our Method	<b>0.571</b>

ing datasets are used for training using our method as compared to training on a single dataset.

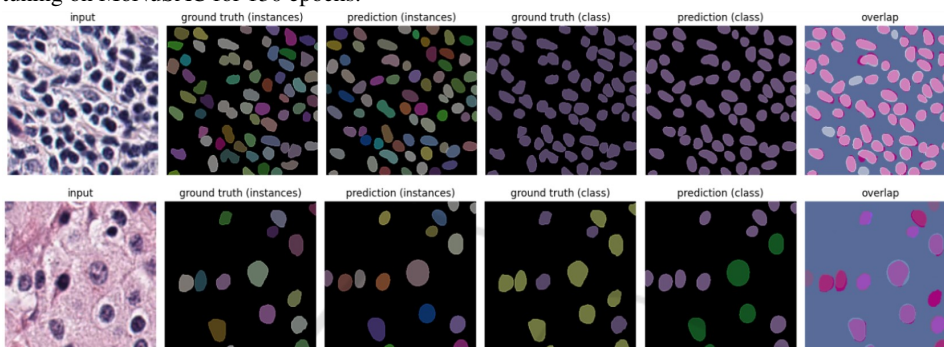
It is worth noting that the improvement is more pronounced when the pretraining dataset is more generalized and has a super-set of classes and organs as compared to the target dataset. For example, the PanNuke dataset has most of the cell classes present in it. Thus, pre-training on PanNuke and then fine-tuning on other more specialized datasets gives significant improvement in the predictions on those datasets. Based on this observation and reasoning, the most general dataset in terms of labels can be chosen for pre-training by surveying the classes of the available open source datasets.

#### 4.2 Evolution of Loss

Figure 3 shows an example of evolution of the losses as the training progressed for the MoNuSAC dataset as the target dataset. When trained only on MoNuSAC (case (a)), the model starts to overfit as it can be seen that the validation loss starts to increase. However, when pretrained on PanNuke (case (b)), the validation loss shows a marked further drop when the dataset is switched to the training subset of MoNuSAC as compared to that of case (a).



(a) Predictions on MoNuSAC of the model pretrained on PanNuke for 250 epochs followed by fine-tuning on MoNuSAC for 130 epochs.



(b) Predictions on MoNuSAC of the model trained on MoNuSAC for 175 epochs before overfitting starts to occur.

Figure 2: A qualitative sample of test split results.

### 4.3 Domain Generalization

To test that domain generalization can improve by training on multiple datasets, we trained the model on the first dataset while monitoring its validation loss to prevent overfitting. After this, we fine-tuned the model on a second dataset. Then we tested on a third dataset, which did not contribute to the training at all. Table 4 summarizes the results of this experiment. Pre-training on a dataset and then fine-tuning for a small number of epochs (Eps) on another dataset gives better results on an unseen dataset as compared to training only on the first dataset. Thus, our model is able to consolidate the knowledge of two datasets.

Table 4: Quantitative results for domain generalization.

Pre-Train	Eps	Fine-tune	Eps	Test	PQ
CoNSeP	100	-	-	MoNuSAC	0.433
CoNSeP	100	PanNuke	62	MoNuSAC	<b>0.563</b>
CoNSeP	100	-	-	PanNuke	0.433
CoNSeP	100	MoNuSAC	43	PanNuke	<b>0.434</b>
MoNuSAC	175	-	-	CoNSeP	0.344
MoNuSAC	175	PanNuke	62	CoNSeP	<b>0.449</b>
MoNuSAC	175	-	-	PanNuke	0.396
MoNuSAC	175	CoNSeP	25	PanNuke	<b>0.405</b>

A sample of qualitative results shown in Figure 4 also shows better overlap between predicted nuclei and annotations for images from an unseen dataset when multiple training datasets are used for training using our method as compared to training on a single dataset.

We can observe that a more pronounced improvement occurs when the fine-tuning dataset is more generalized and has a super-set of classes and organs as compared to the other datasets. We must take care not to use the most generalized dataset (with a super-set of classes) for pretraining because on finetuning with a more specialized dataset, the model loses its accuracy on the unseen dataset instead of benefiting from the fine-tuning. For example, CoNSeP and MoNuSAC are more specialized datasets with classes that have less overlap, but their classes are both subsets of the classes present in PanNuke. In this case, using CoNSeP to finetune the model that was pre-trained on PanNuke will lead to decreased performance on MoNuSAC. Now the most general dataset in terms of labels can be chosen by surveying the classes of the available open source datasets.

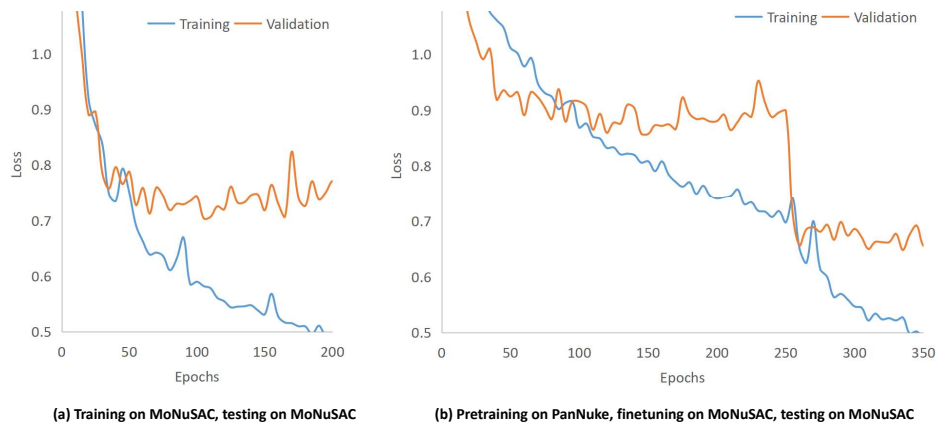
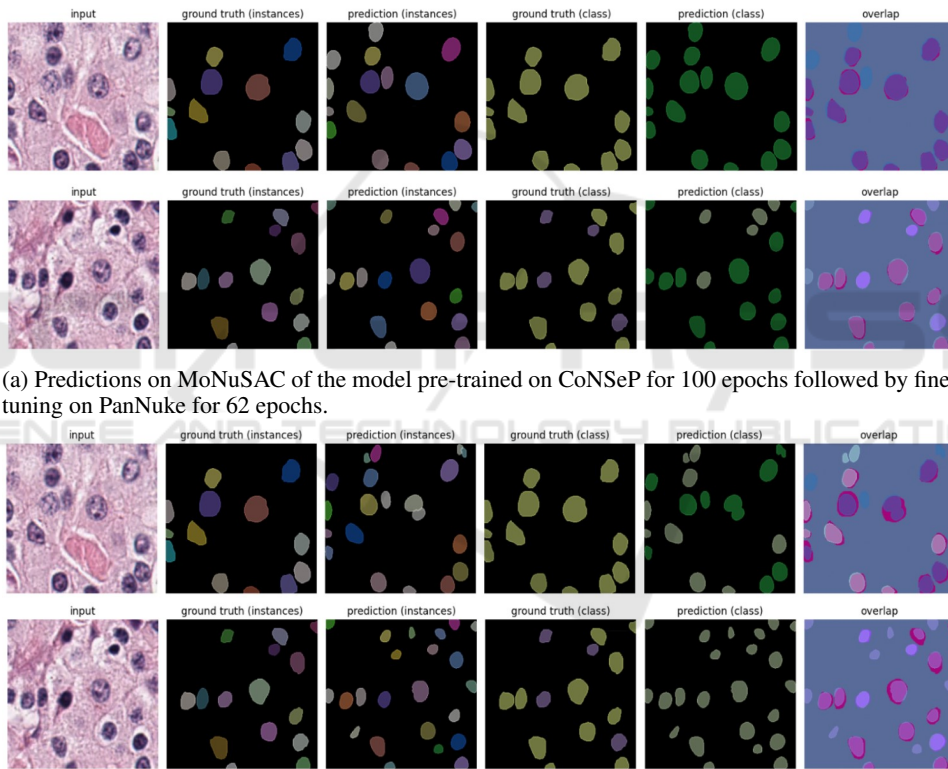


Figure 3: Evolution of training and validation losses for testing on MoNuSAC when (a) trained only on MoNuSAC leading to overfitting, and (b) when pretrained on PanNuke followed by finetuning on MoNuSAC after 250 epochs.



(a) Predictions on MoNuSAC of the model pre-trained on CoNSEP for 100 epochs followed by finetuning on PanNuke for 62 epochs.

(b) Predictions on MoNuSAC of the model trained on CoNSEP for 100 epochs, before overfitting starts to occur.

Figure 4: A qualitative sample of domain generalization results.

## 5 DISCUSSION

We have proposed a method to train a neural network on multiple datasets with different class labels for segmentation and classification. Unlike transfer or multi-task learning, even the last layer is shared between datasets. We achieved this by first creating a hierar-

chical class label tree to relate the class label sets of different datasets to each other as various cuts of the same tree. We then devised a way to combine the losses of the sub-classes, allowing us to train models sequentially on multiple datasets even when the labels are available at a coarser super-class level for some of the classes and datasets. We show improved results

on test splits and unseen datasets. Our technique can easily be applied to other DNN architectures, application domains and tasks (such as, object detection); more importantly, it can also be adapted to other loss functions.

## REFERENCES

- Abdolhoseini, M. et al. (2019). Segmentation of heavily clustered nuclei from histopathological images. *Scientific reports*, 9(1):4551.
- Abraham, N. and Khan, N. M. (2018). A novel focal tversky loss function with improved attention u-net for lesion segmentation.
- Chen, L.-C. et al. (2017). Rethinking atrous convolution for semantic image segmentation.
- Doan, T. N. N. et al. (2022). Gradmix for nuclei segmentation and classification in imbalanced pathology image datasets.
- Dogar, G. M. et al. (2023). Attention augmented distance regression and classification network for nuclei instance segmentation and type classification in histology images. *Biomedical Signal Processing and Control*, 79:104199.
- Gamper, J. et al. (2020). Pannuke dataset extension, insights and baselines.
- Graham, S. et al. (2019). Hover-net: Simultaneous segmentation and classification of nuclei in multi-tissue histology images.
- Kirillov, A. et al. (2019). Panoptic segmentation. In *Proceedings of the IEEE/CVF conference on computer vision and pattern recognition*, pages 9404–9413.
- Kumar, N. et al. (2017). A dataset and a technique for generalized nuclear segmentation for computational pathology. *IEEE transactions on medical imaging*, 36(7):1550–1560.
- Li, Z. et al. (2019). Exploiting coarse-to-fine task transfer for aspect-level sentiment classification. In *Proceedings of the AAAI conference on artificial intelligence*, volume 33, pages 4253–4260.
- Lin, T.-Y. et al. (2017). Focal loss for dense object detection. In *Proceedings of the IEEE International Conference on Computer Vision (ICCV)*.
- Mahbod, A. et al. (2021). Cryonuseg: A dataset for nuclei instance segmentation of cryosectioned h&e-stained histological images. *Computers in biology and medicine*, 132:104349.
- Oh, H.-J. and Jeong, W.-K. (2023). Diffmix: Diffusion model-based data synthesis for nuclei segmentation and classification in imbalanced pathology image datasets.
- Pan, X. et al. (2023). Smile: Cost-sensitive multi-task learning for nuclear segmentation and classification with imbalanced annotations. *Medical Image Analysis*, 88:102867.
- Reis, H. C. and Turk, V. (2023). Transfer learning approach and nucleus segmentation with medcnet colon cancer database. *Journal of Digital Imaging*, 36(1):306–325.
- Ronneberger, O. et al. (2015). U-net: Convolutional networks for biomedical image segmentation. In *Medical Image Computing and Computer-Assisted Intervention–MICCAI 2015: 18th International Conference, Munich, Germany, October 5–9, 2015, Proceedings, Part III 18*, pages 234–241. Springer.
- Schmidt, U., Weigert, M., et al. (2018). Cell detection with star-convex polygons. In *Medical Image Computing and Computer Assisted Intervention – MICCAI 2018*, pages 265–273. Springer International Publishing.
- Sudre, C. H. et al. (2017). Generalised dice overlap as a deep learning loss function for highly unbalanced segmentations. In *Deep Learning in Medical Image Analysis and Multimodal Learning for Clinical Decision Support: Third International Workshop, DLMIA 2017, and 7th International Workshop, ML-CDS 2017, Held in Conjunction with MICCAI 2017, Québec City, QC, Canada, September 14, Proceedings 3*, pages 240–248. Springer.
- Verma, R. et al. (2021). Monusac2020: A multi-organ nuclei segmentation and classification challenge. *IEEE Transactions on Medical Imaging*, 40(12):3413–3423.
- Weigert, M. and Schmidt, U. (2022). Nuclei instance segmentation and classification in histopathology images with stardist. In *2022 IEEE International Symposium on Biomedical Imaging Challenges (ISBIC)*. IEEE.
- Ye, Z. et al. (2024). Dsca-net: Double-stage codec attention network for automatic nuclear segmentation. *Biomedical Signal Processing and Control*, 88:105569.
- Yosinski, J. et al. (2014). How transferable are features in deep neural networks? *Advances in neural information processing systems*, 27.
- Zhang, Z. et al. (2014). Facial landmark detection by deep multi-task learning. In *Computer Vision–ECCV 2014: 13th European Conference, Zurich, Switzerland, September 6–12, 2014, Proceedings, Part VI 13*, pages 94–108. Springer.
- Zhao, H. et al. (2017). Pyramid scene parsing network. In *Proceedings of the IEEE conference on computer vision and pattern recognition*, pages 2881–2890.
- Zhao, T. et al. (2023). Gsn-hvnet: A lightweight, multi-task deep learning framework for nuclei segmentation and classification. *Bioengineering*, 10(3):393.
- Zhou, Z. et al. (2018). Unet++: A nested u-net architecture for medical image segmentation. In *Deep Learning in Medical Image Analysis and Multimodal Learning for Clinical Decision Support: 4th International Workshop, DLMIA 2018, and 8th International Workshop, ML-CDS 2018, Held in Conjunction with MICCAI 2018, Granada, Spain, September 20, 2018, Proceedings 4*, pages 3–11. Springer.